# Spatial Scales of Local Adaptation and Host-Parasite Coevolution

**Bob Week**
Integrative Biology
Michigan State University
East Lansing, MI 48824
bobweek@gmail.com

**Gideon Bradburd**
Integrative Biology
Michigan State University
East Lansing, MI 48824
bradburd@msu.edu

October 4, 2021

## Abstract

Studies of local adaptation between coevolving hosts and parasites have profited from theory that assumes a discrete set of populations. However, when dispersal is limited continuous patterns of phenotypic variation may emerge. Thus, patterns of local adaptation may occur on characteristic spatial scales determined by relative dispersal distances and strengths of selection. Furthermore, neutral patterns of spatial correlation between traits may occur when they are spatially autocorrelated. Hence, theory is needed to understand spatial scales of local adaptation and coevolution and to disentangle the causes of patterns of trait correlations across space. To fill this gap we study a two-dimensional continuous space model of host-parasite coevolution. Our results synthesize theory of host-parasite coevolution, local adaptation and evolution in continuous space by . . . We find that the species with more limited dispersal tend to be locally adapted, but XYZ about it being ahead in the coevolutionary race. To verify our results when model assumptions are broken, we use individual based simulations. We find XYZ about our results when coevolution is strong and XYZ when population densities significantly vary across space.

***K*eywords** host-parasite coevolution · local adaptation · continuous space · characteristic scales · spde

## 1 Introduction

Local adaptation occurs when individuals reared in the same geographic location as their ancestors exhibit higher fitness than when reared elsewhere. This phenomenon is thought to occur (or has been show to occur) when selection is spatially heterogeneous and strong relative to dispersal (refs).

- It seems an old motivation for studying local adaptation in host-parasite coevolution comes from trying to make sense of the GMTC. So I think it would be good to include this.
- Need to do lit review of local adaptation in coevolving host-parasite systems.
- We should also tie in previous work on understand spatial scales of phenotypic variation (ie, Slatkin's 1978 ppr). Need to do lit review in this area too.

## 2 Methods

To understand patterns of phenotypic variation and local adaptation in continuous space, we introduce and analyze a pair of stochastic partial partial differential equations (SPDE) that account for coevolution between host and parasite, abiotic stabilizing selection and random genetic drift. In particular, SPDE are stochastic generalizations of deterministic PDE which in turn have been widely employed in theoretical

evolutionary ecology to study continuous space population dynamics (refs), the evolution of continuous trait distributions (refs) and feedbacks between the two (refs). Here we employ the SPDE framework to model the evolution of mean traits in coevolving hosts and parasites. By assuming additive genetic variances and population sizes are spatially and temporally homogeneous, we arrive at a pair of linear SPDE driven by space-time white noise processes. Linearity of the model allows us to employ spectral methods to approximate spatial auto-covariance functions of mean traits for each species along with a spatial cross-covariance function between the mean traits of the two species. Using the spatial auto-covariance functions, we then identify spatial scales of phenotypic turnover.

In section 2.1 we introduce our model and briefly outline our approach using spectral methods. More information on this approach is provided in Appendix A. We then adapt a classical measure of local adaptation in terms of population growth rates instead of fitness measured as lifetime reproductive output. Using these adapted measures, we apply our model results to illustrate the spatial scales of local adaptation and to determine which species has a coevolutionary advantage. These definitions are provided in section 2.2 and further details are located in Appendix B. To test our analytical results, we employ individual-based simulations conducted in the language Julia (ref). In section 2.3, we provide a brief overview of our simulation model. Further details on the individual-based model can be found in Appendix C

## 2.1 SPDE model

We employ a pair of stochastic partial differential equations to track the evolution of mean traits in the host, $\bar{z}_H(\boldsymbol{x})$, and the parasite, $\bar{z}_P(\boldsymbol{x})$, as functions of the two-dimensional spatial coordinates $\boldsymbol{x} = (x_1, x_2)^\top$. We assume geographical space is unbounded so that $\boldsymbol{x}$ spans the entire plane $\mathbb{R}^2$. We account for the effects of host-parasite coevolution using a trait-matching model (ref other pprs using this model). Under this model, fitness of the host is minimized and fitness of the parasite is maximized when traits are matching. This induces a local coevolutionary chase, where the parasite evolves to match the host, but the host evolves to escape the parasite (this should be stated in the introduction somewhere). The strength of biotic selection (i.e., selection that is induced by the interaction between hosts and parasites) is denoted by $B_H > 0$ for the host and $B_P > 0$ for the parasite. We assume these strengths of selection are temporally and spatially homogeneous. To obtain an equilibrium solution to our model, we also account for the effects of abiotic stabilizing selection. Here, we assume abiotic optimal traits and strengths of abiotic selection for both species are temporally and spatially homogeneous. We denote by $\theta_H, \theta_P$ the abiotic optimal traits and by $A_H, A_P > 0$ the strengths of abiotic stabilizing selection in the host and parasite respectively. Finally, our model also accounts for the effects of limited dispersal by assuming individuals disperse following a bivariate Gaussian distribution with mean zero and equal standard deviations in both directions. We denote by $\sigma_H, \sigma_P > 0$ the standard deviations of individual movement in the host and parasite respectively. In our SPDE model, this translates to diffusion with coefficients $\sigma_H^2/2$ and $\sigma_P^2/2$ (refs). For the sake of mathematical tractability, we also assume the additive genetic variances $G_H, G_P > 0$ and population densities $\rho_H, \rho_P > 0$ are temporally and spatially homogeneous for the host and parasite respectively. In Table X we provide a summary of model parameters. With this notation, our model can be written as

$$\frac{\partial \bar{z}_H}{\partial t} = G_H B_H (\bar{z}_H - \bar{z}_P) + G_H A_H (\theta_H - \bar{z}_H) + \frac{\sigma_H^2}{2} \left( \frac{\partial^2 \bar{z}_H}{\partial x_1^2} + \frac{\partial^2 \bar{z}_H}{\partial x_2^2} \right) + \sqrt{\frac{G_H}{\rho_H}} \dot{W}_H, \tag{1a}$$

$$\frac{\partial \bar{z}_P}{\partial t} = G_P B_P (\bar{z}_H - \bar{z}_P) + G_P A_P (\theta_P - \bar{z}_P) + \frac{\sigma_H^2}{2} \left( \frac{\partial^2 \bar{z}_P}{\partial x_1^2} + \frac{\partial^2 \bar{z}_P}{\partial x_2^2} \right) + \sqrt{\frac{G_P}{\rho_P}} \dot{W}_P. \tag{1b}$$

Here $\dot{W}_H, \dot{W}_P$ denote two independent space-time white noise processes, which are Gaussian processes with values that are independent in both space and time. In particular, integrating $\dot{W}_S$, (for either $S = H$ or $S = P$), over an interval of time $[t_1, t_2]$ and a geographic region $U$ returns a normally distributed random variable with mean zero and variance equal to $(t_2 - t_1)|U|$, where $|U|$ denotes the area of $U$ (refs). Hence, over an interval of unit length and region of unit area, the integral of $\sqrt{G_S/\rho_S}\dot{W}_S$ is normal with mean zero and variance $G_S/\rho_S$ in analogy with classical models of random genetic drift used in quantitative genetic theory (refs). Since every parameter of the model is assumed to be spatially and temporally homogeneous, spatial variation under this model is ultimately caused by random genetic drift.

The assumption of constant effective population size across time and space can be thought of as an extreme form of population regulation. However, the model is agnostic to whether population regulation is caused by top-down forces such as predation, bottom-up forces such as resource competition or some combination

thereof. Similarly, the assumption of constant additive genetic variances can be justified theoretically via mutation-selection balance (refs).

We analyze model (1) at its statistical equilibrium, which exists and is unique when $A_H > B_H$ (see Appendix A). Following well established results of spatial statistics (refs), we know the equilibrium solution of model (1) is a bivariate Gaussian random field (refs for GRFs). An example of an equilibrium solution to model (1) is illustrated in Figure X. A multivariate Gaussian random field of $p$ variables has the convenient property of being characterized by its $p$-dimensional mean vector $\boldsymbol{\mu}(x_1, x_2)$ and $p \times p$ spatial auto/cross-covariance matrix $\boldsymbol{C}(\boldsymbol{x}, \boldsymbol{y})$ (refs). While the (intraspecific) auto-covariance functions for each of the $p$ variables occur along the diagonal of $\boldsymbol{C}(\boldsymbol{x}, \boldsymbol{y})$, the (interspecific) cross-covariance functions occur on the off-diagonal entries representing covariance between different variables at potentially different locations. In particular, the $(i, j)$th entry of $\boldsymbol{C}(\boldsymbol{x}, \boldsymbol{y})$ measures the covariance between the $i$th and $j$th variables sampled at locations $\boldsymbol{x} = (x_1, x_2)$ and $\boldsymbol{y} = (y_1, y_2)$ respectively. Taking expectation of our model at equilibrium, we find $\boldsymbol{\mu}(x_1, x_2) = (\tilde{z}_H, \tilde{z}_P)^\top$ is the vector of expected equilibrium trait values, which are spatially homogeneous and are determined by a balance between biotic and abiotic selection (expressions and derivation are provided in Appendix A).

Obtaining the spatial auto/cross-covariance matrix $\boldsymbol{C}(\boldsymbol{x}, \boldsymbol{y})$ is more challenging. However, since we assume all model parameters are spatio-temporally homogeneous, we can use known results on linear SPDE to conclude that $\boldsymbol{C}(\boldsymbol{x}, \boldsymbol{y})$ is stationary which implies that it only depends on the distance between $\boldsymbol{x}$ and $\boldsymbol{y}$ (refs). Hence, from hereon we write $\boldsymbol{C}(d)$ for some distance $d \geq 0$ between sampled locations. Linearity of the SPDE model (1) and stationarity of the auto/cross-covariance matrix allow us to employ spectral methods and capitalize on the relationship between spatial auto-covariance functions and power spectra of stationary Gaussian random fields. In particular, the power spectrum of a stationary Gaussian random field (where stationarity here implies spatial homogeneity of mean vector and stationarity of auto-covariance function) is the Fourier transform of the spatial auto-covariance function. Denote by $(\hat{z}_H(\boldsymbol{k}), \hat{z}_P(\boldsymbol{k}))^\top = \mathscr{F}\left[(\tilde{z}_H(\boldsymbol{x}), \tilde{z}_P(\boldsymbol{x}))^\top\right]$ the Fourier transformed equilibrium solution to model (1), where $\boldsymbol{k} = (k_1, k_2)$ correspond to spatial frequencies in each direction. The power spectra of the stationary solution to our model can then be computed as $S_H(\boldsymbol{k}) = \mathbb{E}(\hat{z}_H^2(\boldsymbol{k}))$, $S_P(\boldsymbol{k}) = \mathbb{E}(\hat{z}_P^2(\boldsymbol{k}))$ and $S_{HP}(k) = \mathbb{E}(\hat{z}_H(\boldsymbol{k})\hat{z}_P(\boldsymbol{k}))$, where $\mathbb{E}$ denotes expectation across all possible outcomes. Then, by setting $C_H(d), C_P(d)$ equal to the respective spatial auto-covariance functions of the host and parasite mean traits and $C_{HP}(d)$ equal to the spatial cross-covariance function between host and parasite mean traits, we have

$$C_H(d) = \mathscr{F}^{-1}\left[S_H(\boldsymbol{k})\right], \ C_P(d) = \mathscr{F}^{-1}\left[S_P(\boldsymbol{k})\right], \ C_{HP}(d) = \mathscr{F}^{-1}\left[S_{HP}(\boldsymbol{k})\right], \tag{2}$$

where $\mathscr{F}^{-1}$ denotes inverse Fourier transformation. Hence, although directly calculating the matrix of spatial covariance functions $\boldsymbol{C}(d)$ from model (1) is challenging, computing the power spectra and taking their inverse Fourier transforms is straightforward when the power spectra take simple forms. In Appendix A we use a weak coevolution approximation to simplify expressions of power spectra and calculate analytical expressions for the spatial (intraspecific) auto-covariance and (interspecific) cross-covariance functions of host and parasite mean traits. In the next section, we make use of the spatial cross-covariance function $C_{HP}(d)$ to define a measure of local adaptation for species distributed continuously in space.

## 2.2 Local adaptation in continuous space

Measures of local adaptation quantify the difference in average fitness of individuals reared in local environmental conditions versus average fitness of individuals reared in foreign environmental conditions (refs). When individual fitness tends to be greater in local conditions in comparison to foreign conditions, the species is considered to be locally adapted. In this section we introduce a definition of local adaptation for species distributed continuously in space. However, before doing so, we briefly review a classical measure of local adaptation for species distributed in a finite number of discrete locations to motivate our continuous space analog.

Classically, measures of local adaptation are defined for finite, spatially discrete habitats in terms of expected lifetime reproductive output for an average individual transplanted from some locality $i$ to some other locality $j$, denoted here by $\bar{w}_S(i, j)$ for species $S = H, P$. The bar above $w_S$ signifies that we are averaging across trait values of individuals in species $S$ found at location $i$. Then, assuming a finite number $K$ of discrete habitats, average fitness of individuals reared in their local environmental conditions can be captured by $\bar{\bar{w}}_S = \sum_i \bar{w}_S(i, i)/K$ and average fitness of individuals transplanted to a randomly selected location can be captured by $\hat{\bar{w}}_S = \sum_{i,j} \bar{w}_S(i, j)/K^2$, where the sums are taken over $i = 1, \ldots, K$ and $i, j = 1, \ldots, K$ respectively. Then, a commonly used definition of local adaptation is given by $\mathcal{L}_S = \bar{\bar{w}}_S - \hat{\bar{w}}_S$ (refs). In

turn, $\mathcal{L}_S$ can be written in terms of the spatial covariance of host and parasite genotype frequencies (refs) or of host and parasite phenotypic distributions (see Appendix **??**). In particular, this definition implies the parasite species is locally adapted when genotype or phenotype frequencies between host and parasite positively covary across locations. Conversely, the host is locally adapted when this covariance is negative.

To obtain an analogous measure of local adaptation to $\mathcal{L}_S$ for species distributed continuously in space, we consider the difference in Malthusian growth rates for individuals reared in local conditions versus those reared in randomly drawn locations. In particular, we denote by $m_H(z_H, z_P)$ the Malthusian growth rate of host individuals having trait $z_H$ encountering parasite individuals with trait $z_P$. Similarly, $m_P(z_P, z_H)$ is the growth rate of parasite individuals with trait $z_P$ encountering host individuals with trait $z_H$. Setting $\varphi_S(z_S, \boldsymbol{x})$ the frequency of trait value $z_S$ in species $S$ at location $\boldsymbol{x}$, the Malthusian growth rate of hosts transplanted from location $\boldsymbol{x}$ to location $\boldsymbol{y}$ is given by

$$\bar{m}_H(\boldsymbol{x}, \boldsymbol{y}) = \int_{-\infty}^{+\infty} \int_{-\infty}^{+\infty} m_H(z_H, z_P) \varphi_H(z_H, \boldsymbol{x}) \varphi_P(z_P, \boldsymbol{y}) dz_H dz_P. \tag{3}$$

The analogous quantity for the parasite species, $\bar{m}_P(\boldsymbol{x}, \boldsymbol{y})$, can be defined in a similar fashion. Since, under our model (1), mean traits are random variables, the Malthusian growth rates $\bar{m}_H(\boldsymbol{x}, \boldsymbol{y}), \bar{m}_P(\boldsymbol{x}, \boldsymbol{y})$ are also random variables. We therefore define local adaptation in terms of expectations of these growth rates. In particular, we define a geographically specific measure of local adaptation for individuals of species $S$ drawn from location $\boldsymbol{x}$ and transplanted to location $\boldsymbol{y}$ as

$$\Delta_S(\boldsymbol{x}, \boldsymbol{y}) = \mathbb{E}\big[\bar{m}_S(\boldsymbol{x}, \boldsymbol{x}) - \bar{m}_S(\boldsymbol{x}, \boldsymbol{y})\big]. \tag{4}$$

Since our model of mean trait evolution described in section 2.1 implies $(\bar{z}_H(\boldsymbol{x}), \bar{z}_P(\boldsymbol{x}))^\top$ is a stationary, isotropic Gaussian random field, $\bar{m}_S(\boldsymbol{x}, \boldsymbol{y})$ and $\Delta_S(\boldsymbol{x}, \boldsymbol{y})$ depend only on the distance $d \geq 0$ between locations $\boldsymbol{x}$ and $\boldsymbol{y}$ for both host and parasite. We therefore write $\bar{m}_S(d) = \bar{m}_S(\boldsymbol{x}, \boldsymbol{y})$ and $\Delta_S(d) = \Delta_S(\boldsymbol{x}, \boldsymbol{y})$ when the distance between $\boldsymbol{x}$ and $\boldsymbol{y}$ is $d$. Furthermore, since we model host and parasite species as being distributed continuously across the entire plane $\mathbb{R}^2$, the assumption that the location transplanted to is drawn uniformly at random (consistent with the classical measure $\mathcal{L}_S$) implies the distance transplanted will almost surely be infinite. We therefore define our continuous space analog of local adaptation for species $S$ distributed in unbounded habitats as

$$\ell_S^\infty = \lim_{d \to \infty} \Delta_S(d). \tag{5}$$

In section **??** we present results found by combining our definition of local adaptation in continuous space with our model of host-parasite coevolution. Although this definition and analytical results presented below have relatively simple expressions, they come at the cost of several important model assumptions. We therefore developed individual-based simulations to relax these key assumptions. In the following section, we describe the structure of our individual-based simulations and approach taken to analyze simulated output for comparison with results found using the SPDE model (1).

## 2.3   Relaxing model assumptions

To understand the robustness of our results, we developed individual-based simulations that relax key model assumptions. In particular, we investigated the consequences of relaxing the assumptions of weak coevolution and unbounded habitat along with spatio-temporally homogeneous population densities, additive genetic variances and abiotic optimal trait values. In this section we begin by describing the structure of our individual-based models, our approach taken to implement or relax key assumptions and methods used to assess the robustness of our analytical results.

### 2.3.1   Individual-based simulations

In each of our individual-based simulations, we track the dynamics of host and parasite species consisting of a finite number of individuals distributed on the unit square. We assume discrete, non-overlapping generations so that time can be measured in integral steps. At the beginning of each generation, we accumulate consequences of intra and interspecific interactions on the fitness of individuals. In particular, we assume a spatial competition model where individual fitness is reduced multiplicatively by an amount $0 < \kappa_S < 1$

for each conspecific within a radius $R_S > 0$, where both of these parameters depend on the species $S$. For example, if the base fitness of a host individual located at $\boldsymbol{x}$ is $w$ and there are $n$ other hosts within $R_H$ of $\boldsymbol{x}$, the resulting fitness of this host individual after spatial competition is $w' = w \times (\kappa_H)^n$. Interspecific interactions between host and parasite individuals are modeled in a similar fashion. We assume parasites choose a single host at random from within a radius $R_\iota > 0$ of the focal parasite location. The probability of infection $\pi(z_H, z_P)$ is determined by the degree to which host and parasite traits match, with a maximum probability of infection $\pi_{\max} > 0$ occurring when $z_H = z_P$. The rate at which the probability of infection decays with $|z_H - z_P|$ is mediated by $\gamma > 0$. When infection fails, we assume no consequences for the fitnesses of individuals involved. In the case of successful infection, we assume the host incurs a fitness cost of $0 < \iota_H < 1$ and the parasite receives a fitness benefit of $\iota_P > 1$. To decouple the effects of spatial competition from coevolution, we allow multiple parasites to infect the same host. Then, given a base fitness of $w$ for a host individual being infected by $n$ parasites, the updated host fitness becomes $w' = w \times (\iota_H)^n$. Finally, we incorporate abiotic stabilizing selection on each species. In particular, individuals accumulate multiplicative fitness effect $\mathscr{A}_S(z_S, \theta_S)$ that depends on the difference $|z_S - \theta_S|$ where $\theta_S$ is the abiotic optimal trait for species $S$ and may depend on geographical location. The maximum fitness effect due to the abiotic environment is $\alpha_S > 0$ and occurs when $z_S = \theta_S$. The rate at which $\mathscr{A}_S(z_S, \theta_S)$ decays with $|z_S - \theta_S|$ is mediated by $A_S > 0$. Before fitness effects are accumulated, we assume all host and parasite individuals begin with a base fitness of one. Population densities can be controlled by tuning the fitness effects of spatial competition $\kappa_H, \kappa_P$, interspecific interactions $\iota_H, \iota_P$, the maximum fitness effects of abiotic selection $\alpha_H, \alpha_P$ and the interaction radii $R_H, R_P, R_\iota$.

At the end of each generation each individual is replaced by a random number of offspring. In particular, for an individual that has accumulated a fitness of $w$, the number of offspring is drawn from a Poisson distribution with mean $w$. Trait values of offspring are normally distributed around parental values with variance $\mu_S$ for species $S$. For simplicity, we assume traits are perfectly heritable. Geographical locations of individuals are also normally distributed (bivariate normal in particular) around parental locations with standard deviation in each direction $\sigma_S$ for species $S$. If an offspring location falls outside the unit square, one of three possibilities occur depending on the boundary conditions chosen. For absorbing boundary conditions, the offspring is removed from the population. For reflecting boundary conditions, the offspring bounces off the habitat boundary with symmetric angles of incidence and reflection. Multiple bounces are possible until the offspring travels the same distance as it would in the absence of boundaries. In the case of periodic boundaries, an offspring that falls off the edge of the habitat appears on the opposite side as if the habitat boundaries were connected to form a torus. Note that spatial competition prevents the famed *pain in the torus* problem (refs). The boundary conditions chosen (e.g., absorbing, reflecting or periodic) for a given simulation depended on whether or not that simulation was developed for investigating the effects of geographically bounded habitats.

This concludes the general description of our simulation model. Further details can be found in Appendix **??** (including details on spatially heterogeneous abiotic optima). Simulation model parameters are summarized in Table Y. Code for simulations were written in the language *Julia* (Bezanson et al. 2017) and can be found in the github repository `https://github.com/bobweek/continuous-space-coevolution`. In the next subsection, we describe our use of this simulation model to check the robustness of our analytical results.

### 2.3.2 Assessing robustness of analytical results

To assess the robustness of our analytical results in face of broken assumptions, we quantified spatial scales of phenotypic turnover and local adaptation for populations simulated for 1000 generations. We then compared the simulated results to analytical results. In particular, to simplify comparison with analytical results, we fitted Matérn spatial correlation functions to simulated trait data separately for each species. To do this, we first implemented a non-parametric estimator of the spatial correlation function using the $R$ package `ncf` (Bjørnstad and Bascompte 2001). We then used the $R$ function `optim` to find a least squares approximation of the non-parametric estimator across all parameter combinations of the Matérn correlation functions. Matérn correlation functions are parameterized by a characteristic length $\xi$ and a roughness parameter $\nu$. Hence, this approach allowed us to estimate characteristic lengths of phenotypic turnover for direct comparison with analytical results. However, before making such comparisons we first assessed whether a Matérn correlation function adequately describes the simulated data using a randomization test. In the case that the simulated data significantly differed from a Matérn correlation function, we concluded that our analytical result failed for that region of model parameters and set of assumptions broken. In the case that the simulated did not significantly differ from a Matérn correlation function, we then used a randomization test to determine

whether or not the analytically predicted spatial scale of phenotypic turnover is a good approximation of the simulated spatial scale of phenotypic turnover. We did this for each species separately.

Next, we tested our results on local adaptation and coevolutionary advantage.

## 3  Results

### 3.1  Spatial covariances and characteristic lengths of phenotypic turnover

Using a weak coevolution approximation to simplify expressions for the power spectra (see Appendix A), we were able to employ an inverse Fourier transform to obtain analytic expressions for the (intraspecific) spatial auto-covariance and (interspecific) spatial cross-covariance functions of host and parasite mean trait values. In particular, we find spatial auto-covariance functions for the host and parasite respectively taking the forms

$$C_H(d) \approx \sqrt{2} V_H \frac{d}{\xi_H} K_1 \left( \sqrt{2} \frac{d}{\xi_H} \right), \tag{6a}$$

$$C_P(d) \approx \sqrt{2} V_P \frac{d}{\xi_P} K_1 \left( \sqrt{2} \frac{d}{\xi_P} \right), \tag{6b}$$

where $V_H, V_P$ are the collocated variances (i.e., $C_S(0) = V_S$ for $S = H, P$), $\xi_H, \xi_P$ are the characteristic lengths of phenotypic turnover across geographic space in each species and $K_\nu(d)$ is a modified Bessel function of second order, degree $\nu$ (ref aboromitz). These spatial covariance functions belong to the class of Matérn covariance functions which have been widely employed in the fields of spatial statistics (refs) and machine learning (refs).

The collocated variances $V_H, V_P$ represent uncertainty in mean trait value at any particular location as opposed to variance of trait values among individuals at that location. Since solutions to our model are spatially homogeneous random fields (i.e., they have the same statistical properties at any given spatial location), mean traits of species $S$ (where $S = H$ or $S = P$) at locations separated by distances much greater than the characteristic length $\xi_S$ return essentially independent and identically distributed random variables with variances equal to the collocated variance $V_S$. Thus, the collocated variances also provide measures of global diversity of mean traits across space. In terms of our model parameters, the collocated variances can be expressed as

$$V_H = \frac{1}{\rho_H \sigma_H^2 (A_H - B_H)}, \quad V_P = \frac{1}{\rho_P \sigma_P^2 (A_P + B_P)}. \tag{7}$$

From the expressions for $V_H$ and $V_P$ we see population density $\rho_S$, dispersal distance $\sigma_S$ and strength of abiotic stabilizing selection $A_S$ all tend to decrease the overall diversity of mean traits of species $S$ across space. Since our model assumes the ultimate source of spatial variation in mean traits is random genetic drift, this explains why increased population density erodes spatial diversity. Similarly, since we assume space extends across the entire plane $\mathbb{R}^2$, in the limit of infinite dispersal distance we arrive at a panmictic population of infinite size, explaining why increased $\sigma_S$ decreases $V_S$. These two results mirror those found in studies of continuous space population genetics using Wright's neighborhood size $\mathscr{N}_S = 4\pi \rho_S \sigma_S$, which is a continuous space analog of effective population size (refs). Since the abiotic optima $\theta_H, \theta_P$ are assumed to be spatially homogeneous, abiotic stabilizing selection around these optima erodes spatial variation of mean traits in both species. In contrast, biotic selection has opposing effects on the degree of spatial variation in host and parasite mean traits. In particular, while increased biotic selection erodes spatial diversity of mean traits for the parasite species since it is stabilizing under the trait-matching model, increased biotic selection on the host promotes spatial variation because it is disruptive under the trait-matching model. However, since we require abiotic stabilizing selection on the host to outweigh biotic disruptive selection (i.e., $A_H > B_H$) for the existence of equilibrium solutions, selection will be overall stabilizing for both species around augmented optima that strike a balance between biotic and abiotic selection (see Appendix A). In turn, since these augmented optima are spatially homogeneous, the overall stabilizing effect of selection diminishes the magnitude of spatial variation in mean traits for both species.

The characteristic lengths of phenotypic turnover across space in the host and parasite can be expressed in terms of model parameters respectively as

$$\xi_H = \frac{\sigma_H}{\sqrt{G_H(A_H - B_H)}}, \; \xi_P = \frac{\sigma_P}{\sqrt{G_P(A_P + B_P)}}. \tag{8}$$

From these expressions, we see that characteristic spatial scales of phenotypic variation are proportional to the standard deviations of dispersal distances in the respective species. Hence, the further individuals tend to move, the larger the spatial scales one must observe to see significant phenotypic variation. We also see that increased additive genetic variance and abiotic stabilizing selection tends to decrease these spatial scales in each species. This reduction in spatial scale by additive genetic variance can be explained by the fact that additive genetic variation inflates the effects of random genetic drift, here assumed to be the ultimate source of spatial variation. With increased spatial variation, one can observe significant changes in mean trait values over shorter spatial scales. However, since stabilizing selection homogenizes mean trait values across space, it is less obvious why increased strength of abiotic selection should decrease spatial scales of phenotypic turnover.

In contrast to the relatively simple expressions for the intraspecific auto-covariance functions, the expression for the interspecific cross-covariance function is rather cumbersome. In particular, $C_{HP}(d)$ can be approximated as the difference of two convolutions when coevolution is weak, the expression for which is provided in Appendix A. However, our measure of local adaptation (eqn. 13) requires only the collocated covariance $C_{HP}(0)$. We can therefore sidestep calculating the cross-covariance $C_{HP}(d)$ for $d > 0$. The collocated covariance $C_{HP}(0)$ can be obtained via spectral methods and the calculations for which are provided in Appendix A. In particular, we find

$$C_{HP}(0) \approx \frac{G_H G_P}{\sigma_H^2 \sigma_P^2} \frac{\xi_H^2 \xi_P^2}{(\xi_H^2 - \xi_P^2)^2} \left[ \frac{B_P}{\rho_H \sigma_H^2} \left( \xi_H^4 + \xi_H^2 \xi_P^2 (\ln \xi_P^2 - \ln \xi_H^2 - 1) \right) \right.$$
$$\left. - \frac{B_H}{\rho_P \sigma_P^2} \left( \xi_P^4 + \xi_H^2 \xi_P^2 (\ln \xi_H^2 - \ln \xi_P^2 - 1) \right) \right]. \tag{9}$$

In analogy to how the collocated variances $V_H, V_P$ provide global measures of mean trait variation across space within each species, the collocated covariance $C_{HP}(0)$ provides a global measure of mean trait co-variation across space between the two species. Expression (9) implies that, when hosts and parasites exhibit approximately equal spatial scales of phenotypic turnover (i.e., when $\xi_H \approx \xi$ and $\xi_P \approx \xi$ for some $\xi > 0$), the collocated covariance is approximately

$$C_{HP}^{(\xi_H \approx \xi_P)}(0) \approx \frac{\xi^4}{2} G_H G_P \left( \frac{B_P}{\rho_H \sigma_H^4 \sigma_P^2} - \frac{B_H}{\rho_P \sigma_H^2 \sigma_P^4} \right). \tag{10}$$

Hence, in this limiting case, we see that increased biotic selection on the parasite over the host ($B_P > B_H$) tends to increase spatial covariance of host and parasite mean traits. We also see spatial covariance increases when the parasite population density is greater than the host population density ($\rho_P > \rho_H$) and when parasite dispersal distance exceeds host dispersal distance ($\sigma_P > \sigma_H$) under the condition that $\sigma_H, \sigma_P > 1$.

We can also investigate the collocated covariance under two other extremes; when the spatial scale of phenotypic turnover for the host is much less than the scale of phenotypic turnover in the parasite, so that $\xi_H \ll \xi_P$, and when this relationship is reversed so that $\xi_P \ll \xi_H$. For $\xi_H \ll \xi_P$ and $\xi_P \ll \xi_H$ respectively, second order Taylor expansion yields

$$C_{HP}^{(\xi_H \ll \xi_P)}(0) \approx -\frac{B_H}{(A_H - B_H)(A_P + B_P)\sigma_P^2 \rho_P}, \; C_{HP}^{(\xi_P \ll \xi_H)}(0) \approx \frac{B_P}{(A_H - B_H)(A_P + B_P)\sigma_H^2 \rho_H}. \tag{11}$$

From these two limiting cases we see the collocated spatial covariance is always negative when $\xi_P \ll \xi_H$ and always positive when $\xi_P \ll \xi_H$. The collocated spatial correlation is given by $C_{HP}(0)/\sqrt{V_H V_P}$ and can therefore be approximated by combining expressions (7) and (11). In the next section we capitalize on these results to understand patterns of host and parasite local adaptation.

## 3.2 Local adaptation

Recall that $\Delta_S(d)$ is the differences in fitness (measured as population growth rates) for individuals of species $S = H, P$ reared in their local environment versus individuals transplanted at some distance $d$. In Appendix

**??** we show that the trait-matching model of fitness used to obtain the mean trait dynamics described by equation (1) implies that $\Delta_H(d)$ and $\Delta_P(d)$, the difference in growth rates for respective host or parasite individuals reared in local environment versus those transplanted a distance $d$, can be simplified to

$$\Delta_H(d) = B_H\big(C_{HP}(d) - C_{HP}(0)\big) \tag{12a}$$

$$\Delta_P(d) = B_P\big(C_{HP}(0) - C_{HP}(d)\big). \tag{12b}$$

Finally, since under our model of host-parasite coevolution the cross-covariance function $C_{HP}(d)$ decays to zero as $d \to \infty$, our measure of local adaptation for each species simplifies to

$$\ell_H = -B_H C_{HP}(0), \tag{13a}$$

$$\ell_P = B_P C_{HP}(0). \tag{13b}$$

From equations (13), we see that the host is locally adapted ($\ell_H > 0$) when host and parasite mean traits are negatively correlated across sufficiently long distances (i.e., when $C_{HP}(0) < 0$) and that the parasite is locally adapted when mean traits are positively correlated across sufficiently long distances, where sufficiently long distances here correspond to distances at which intraspecific spatial autocorrelations of mean trait values are negligible. Hence, this definition is consistent with the classical measure $\mathcal{L}_S$ defined for species distributed across discrete patches.

## 4 Discussion

In the absence of biotic selection, our expressions for the characteristic lengths of phenotypic turnover across space (eqns. 8) coincide with the characteristic length found by Slatkin (1978) in his pioneering work on the evolution of quantitative traits in continuous space. Notably, while Slatkin assumed one-dimensional space and discrete time, we assume two-dimensional space and continuous time. Furthermore, while Slatkin assumed spatial variation in mean traits were the result of spatially varying abiotic stabilizing selection, we assume the ultimate source of spatial variation is due to the effects of random genetic drift. Whether or not this coincidence sheds light on some universal property of phenotypic variation across space or is merely a mathematical artifact due to the approximation schemes employed remains unclear.

Limitations of our approach include the assumption of weakly coevolving hosts and parasites, spatially homogeneous abiotic trait optima, strengths of selection, additive genetic variances and abundance densities. Furthermore, in order for our model to have equilibrium solutions, we require abiotic selection to be greater than biotic selection (i.e., $A_H > B_H$).

## 5 Conclusion

# Appendix

## A   Calculating the covariance and cross-covariance functions

Assuming the system has reached a statistical equilibrium, we make use of a Fourier transform convert the model from geographic coordinates to frequency coordinates, where the Fourier transformed solution represents the spatial harmonic content of the solution to the SPDE model. We then use the Fourier transformed model to construct so-called power spectra of the solution, which are exactly the Fourier transformed spatial auto-covariance functions. We then use a weak coevolution approximation to simplify the power spectra so they can be inverted, arriving at analytical expressions for the spatial auto-covariance functions. In turn, the functional form of the spatial auto-covariance functions allows the identification of spatial scales of phenotypic turnover.

To compute formula for the spatial (intraspecific) covariance and (interspecific) cross-covariance functions, we make use of the relation between the covariance functions and power spectra of random fields. In particular, the power spectrum of a multivariate stationary random field $\boldsymbol{F}(\boldsymbol{x})$, $\boldsymbol{x} = (x_1, x_2)$ being spatial location, is defined by $S_{\boldsymbol{F}}(\boldsymbol{k}) = \mathbb{E}\left(\hat{\boldsymbol{F}}(\boldsymbol{k})\hat{\boldsymbol{F}}(\boldsymbol{k})^H\right)$ where $\hat{\boldsymbol{F}}(\boldsymbol{k})$ is the Fourier transform of $\boldsymbol{F}$, the symbol $^H$ denotes Hessian transpose and $\boldsymbol{k} = (k_1, k_2)$ are the Fourier transformed coordinates which represent the frequencies of fluctuations across the two spatial dimensions. Hence, $\hat{\boldsymbol{F}}$ represents the harmonic content of the process $\boldsymbol{F}$. The spatial covariance function $C_{\boldsymbol{F}}(\boldsymbol{x})$ is just the inverse Fourier transform of the power spectrum $S_{\boldsymbol{F}}(\boldsymbol{k})$.

Working with the power spectrum has the advantage of converting differential equations into algebraic equations, making for a more analytically tractable approach. Furthermore, due to the Fourier relationship between $C_{\boldsymbol{F}}(\boldsymbol{x})$ and $S_{\boldsymbol{F}}(\boldsymbol{k})$, we have the convenient properties $\int_{\mathbb{R}^2} C_{\boldsymbol{F}}(\boldsymbol{x})d\boldsymbol{x} = S_{\boldsymbol{F}}(\boldsymbol{0})$ and $\int_{\mathbb{R}^2} S_{\boldsymbol{F}}(\boldsymbol{x})d\boldsymbol{x} = C_{\boldsymbol{F}}(\boldsymbol{0})$. Both of these properties will aid in calculating results on host-parasite local adaptation.

Using $\boldsymbol{k} = (k_1, k_2)$ to denote spatial frequency (the Fourier equivalent to spatial location $\boldsymbol{x} = (x_1, x_2)$) and $\hat{\boldsymbol{z}}(\boldsymbol{k}) = (\hat{z}_H(\boldsymbol{k}), \hat{z}_P(\boldsymbol{k}))^\top$ to denote the Fourier transforms of the equilibrium solution $\bar{\boldsymbol{z}}(\boldsymbol{x}) = (\bar{z}_H(\boldsymbol{x}), \bar{z}_P(\boldsymbol{x}))^\top$, the Fourier transform of our model at equilibrium is

$$0 = G_H A_H(\theta_H - \hat{z}_H) - G_H B_H(\hat{z}_P - \hat{z}_H) - \frac{\sigma_H^2}{2}\|\boldsymbol{k}\|^2 \hat{z}_H + \sqrt{\frac{G_H}{N_H}}\widehat{\dot{W}}_H,$$

$$0 = G_P A_P(\theta_P - \hat{z}_P) + G_P B_P(\hat{z}_H - \hat{z}_P) - \frac{\sigma_P^2}{2}\|\boldsymbol{k}\|^2 \hat{z}_P + \sqrt{\frac{G_P}{N_P}}\widehat{\dot{W}}_P,$$

where $\|\boldsymbol{k}\|^2 = k_1^2 + k_2^2$ and $\widehat{\dot{W}}_S$ is a heuristic representation for the Fourier transform of the spatial white noise $\dot{W}_S$ for species $S = H, P$. Since the mean vector for equilibrium solution of the SPDE model is spatially homogeneous, we set $\theta_H = \theta_P = 0$ without loss of generality. This is equivalent to centering the solution by working with $\tilde{z}_H = \bar{z}_H - \mu_H$ and $\tilde{z}_P = \bar{z}_P - \mu_P$ instead of $\bar{z}_H$ and $\bar{z}_P$. The Fourier transformed SPDE model can be rewritten in matrix form as

$$\mathscr{H}\hat{\boldsymbol{z}} = \widehat{\dot{\boldsymbol{W}}}$$

where $\widehat{\dot{\boldsymbol{W}}} = \frac{1}{2\pi}\left(-\sqrt{\frac{G_H}{N_H}}\hat{\dot{W}}_H, -\sqrt{\frac{G_P}{N_P}}\hat{\dot{W}}_P\right)^\top$ and

$$\mathscr{H} = \frac{1}{2\pi}\begin{pmatrix} -G_H A_H + G_H B_H + \frac{\sigma_H^2}{2}\|\boldsymbol{k}\|^2 & -G_H B_H \\ G_P B_P & -G_P A_P - G_P B_P + \frac{\sigma_P^2}{2}\|\boldsymbol{k}\|^2 \end{pmatrix}.$$

Since no complex numbers appear in the above expressions, the power spectrum of the random field $\bar{\boldsymbol{z}}$ simplifies to $S_{\bar{\boldsymbol{z}}} = \mathbb{E}\left(\hat{\boldsymbol{z}}\hat{\boldsymbol{z}}^\top\right)$. Rearranging the above matrix equation, we find

$$\hat{\boldsymbol{z}} = \mathscr{H}^{-1}\widehat{\dot{\boldsymbol{W}}},$$

$$\hat{\boldsymbol{z}}^\top = \widehat{\dot{\boldsymbol{W}}}^\top \left(\mathscr{H}^\top\right)^{-1}.$$

Hence, the power spectrum of $\bar{\boldsymbol{z}}$ is

$$S_{\bar{\boldsymbol{z}}} = \mathscr{H}^{-1} S_{\dot{\boldsymbol{W}}} \left(\mathscr{H}^\top\right)^{-1}$$

where

$$S_{\dot{\boldsymbol{W}}} = \mathbb{E}\left(\widehat{\dot{\boldsymbol{W}}}\widehat{\dot{\boldsymbol{W}}}^\top\right) = \frac{1}{(2\pi)^2}\begin{pmatrix} G_H/N_H & 0 \\ 0 & G_P/N_P \end{pmatrix}$$

is the power spectrum of the spatial white noise $\dot{\boldsymbol{W}} = \left(-\sqrt{\frac{G_H}{N_H}}\dot{W}_H, -\sqrt{\frac{G_P}{N_P}}\dot{W}_P\right)^\top$. Denoting $S_H, S_P$ and $S_{HP}$ the components of $S_{\bar{\boldsymbol{z}}}$ corresponding to the host power spectrum, parasite power spectrum and host-parasite cross-power spectrum we find

$$S_H(\boldsymbol{k}) = \frac{B_H^2 G_H^2 \frac{G_P}{N_P} + \frac{G_H}{N_H}\left[G_P(A_P + B_P) + \frac{1}{2}\sigma_P^2\|\boldsymbol{k}\|^2\right]^2}{\left\{B_H B_P G_H G_P + [G_H(A_H - B_H) + \frac{1}{2}\sigma_H^2\|\boldsymbol{k}\|^2][G_P(A_P + B_P) + \frac{1}{2}\sigma_P^2\|\boldsymbol{k}\|^2]\right\}^2},$$

$$S_P(\boldsymbol{k}) = \frac{B_P^2 G_P^2 \frac{G_H}{N_H} + \frac{G_P}{N_P}\left[G_H(A_H - B_H) + \frac{1}{2}\sigma_H^2\|\boldsymbol{k}\|^2\right]^2}{\left\{B_H B_P G_H G_P + [G_H(A_H - B_H) + \frac{1}{2}\sigma_H^2\|\boldsymbol{k}\|^2][G_P(A_P + B_P) + \frac{1}{2}\sigma_P^2\|\boldsymbol{k}\|^2]\right\}^2},$$

$$S_{HP}(\boldsymbol{k}) = \frac{B_P G_P \frac{G_H}{N_H}\left[G_P(A_P + B_P) + \frac{1}{2}\sigma_P^2\|\boldsymbol{k}\|^2\right] - B_H G_H \frac{G_P}{N_P}\left[G_H(A_H - B_H) + \frac{1}{2}\sigma_H^2\|\boldsymbol{k}\|^2\right]}{\left\{B_H B_P G_H G_P + [G_H(A_H - B_H) + \frac{1}{2}\sigma_H^2\|\boldsymbol{k}\|^2][G_P(A_P + B_P) + \frac{1}{2}\sigma_P^2\|\boldsymbol{k}\|^2]\right\}^2}.$$

Assuming coevolution is weak so that $B_H^2, B_P^2, B_H B_P \approx 0$, we obtain the approximations

$$S_H(\boldsymbol{k}) \approx \frac{G_H/N_H}{\left(G_H(A_H - B_H) + \frac{\sigma_H^2}{2}\|\boldsymbol{k}\|^2\right)^2}, \quad S_P(\boldsymbol{k}) \approx \frac{G_P/N_P}{\left(G_P(A_P + B_P) + \frac{\sigma_P^2}{2}\|\boldsymbol{k}\|^2\right)^2}$$

$$S_{HP}(\boldsymbol{k}) \approx \frac{B_P G_H G_P/N_H}{\left(G_H(A_H - B_H) + \frac{\sigma_H^2}{2}\|\boldsymbol{k}\|^2\right)^2 \left(G_P(A_P + B_P) + \frac{\sigma_P^2}{2}\|\boldsymbol{k}\|^2\right)}$$

$$-\frac{B_H G_H G_P/N_P}{\left(G_H(A_H - B_H) + \frac{\sigma_H^2}{2}\|\boldsymbol{k}\|^2\right) \left(G_P(A_P + B_P) + \frac{\sigma_P^2}{2}\|\boldsymbol{k}\|^2\right)^2}.$$

In Figure 1, we compare these approximations to the exact power spectra for varying strengths of coevolutionary selection.

To simplify notation, we denote by $\xi_S$ the characteristic scale of spatial trait covariance within species $S = H, P$ and by $V_S$ the marginal variance of the same species. The marginal variance $V_S$ can be thought of as a measure of uncertainty when observing local mean traits. Setting

$$\xi_H = \frac{\sigma_H}{\sqrt{G_H(A_H - B_H)}}, \quad \xi_P = \frac{\sigma_P}{\sqrt{G_P(A_P + B_P)}},$$

$$V_H = \frac{1}{N_H \sigma_H^2(A_H - B_H)}, \quad V_P = \frac{1}{N_P \sigma_P^2(A_P + B_P)},$$

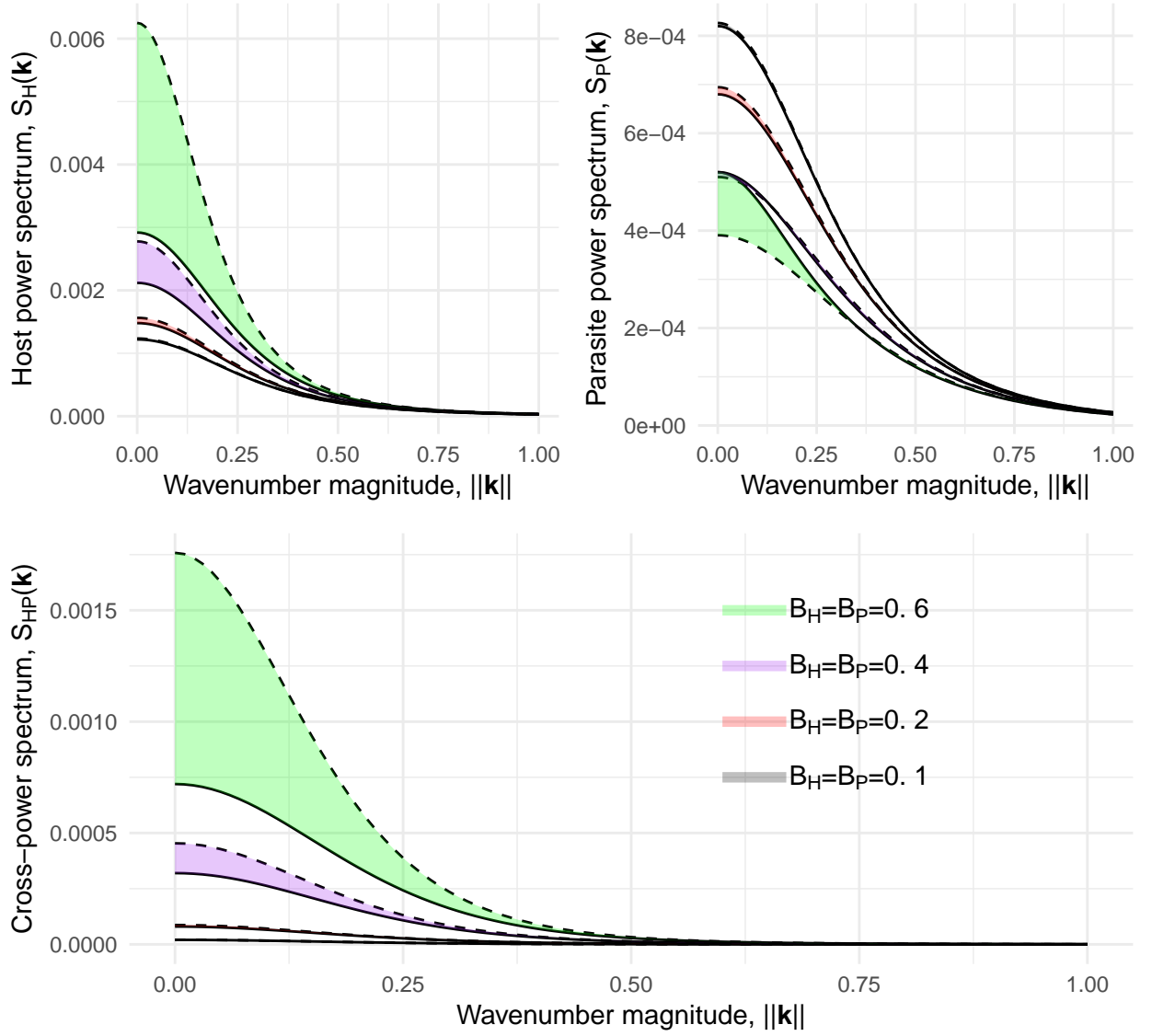the approximated power spectra can be rewritten as

Figure 1: Comparisons of approximated power spectra (dashed lines) to exact power spectra (solid lines) for four different strengths of biotic (coevolutionary) selection $B = 0.1, 0.2, 0.4, 0.6$. For simplicity, biotic selection on host and parasite are set equal ($B_H = B_P = B$). Background parameters are set to $A_H = A_P = 1$, $G_H = G_P = 10$, $\sigma_H = \sigma_P = 10$ and $N_H = N_P = 100$. Our model only is defined for $B_H < A_H$. Hence, the behaviour of power spectra as $B$ increases reflects what happens when the host comes closer to being able to overcome abiotic stabilizing selection and escape parasitism. In this limit, we see that our approximations over estimate the magnitudes of low frequency content in the host spatial covariance and host-parasite cross-covariance. This implies that our approximations over estimate the spatial scale of phenotypic covariance of the host and phenotypic cross-covariance of the host and parasite when coevolution is strong. In contrast, we see that our approximations under estimate the amount of low frequency content in the spatial covariance of parasite traits. This implies that our approximations under estimate the spatial scale of phenotypic covariance of the parasite when coevolution is strong. However, when coevolution is relatively weak, say one-tenth the strength of abiotic selection, we see our approximation matches closely the exact power spectra.

$$S_H(\boldsymbol{k}) \approx \frac{V_H \xi_H^2}{(1 + \frac{1}{2}\xi_H^2 \|\boldsymbol{k}\|^2)^2}, \quad S_P(\boldsymbol{k}) \approx \frac{V_P \xi_P^2}{(1 + \frac{1}{2}\xi_P^2 \|\boldsymbol{k}\|^2)^2}$$

$$S_{HP}(\boldsymbol{k}) \approx \frac{B_P}{A_P + B_P} \frac{1}{1 + \frac{1}{2}\xi_P^2 \|\boldsymbol{k}\|^2} \frac{V_H \xi_H^2}{(1 + \frac{1}{2}\xi_H^2 \|\boldsymbol{k}\|^2)^2} - \frac{B_H}{A_H - B_H} \frac{1}{1 + \frac{1}{2}\xi_H^2 \|\boldsymbol{k}\|^2} \frac{V_P \xi_P^2}{(1 + \frac{1}{2}\xi_P^2 \|\boldsymbol{k}\|^2)^2}.$$

The spatial covariance functions, equal to the inverse Fourier transforms of the power spectra $S_H(\boldsymbol{k}), S_P(\boldsymbol{k}), S_{HP}(\boldsymbol{k})$, can then be approximated as

$$C_H(\boldsymbol{x}) \approx V_H \sqrt{2} \frac{\|\boldsymbol{x}\|}{\xi_H} K_1 \left( \sqrt{2} \frac{\|\boldsymbol{x}\|}{\xi_H} \right),$$

$$C_P(\boldsymbol{x}) \approx V_P \sqrt{2} \frac{\|\boldsymbol{x}\|}{\xi_P} K_1 \left( \sqrt{2} \frac{\|\boldsymbol{x}\|}{\xi_P} \right),$$

where $K_\nu$ is a modified Bessel function of the second kind, order $\nu$. Conveniently, the approximated spatial covariance functions take the form of Whittle-Matérn covariance functions, which are widely applied in the fields of spatial statistics (refs) and machine learning (ref). In general, the Whittle-Matérn covariance function takes the form

$$M_\nu(\boldsymbol{x}|\xi, V) = V \frac{2^{1-\nu}}{\Gamma(\nu)} \left( \sqrt{2\nu} \frac{\|\boldsymbol{x}\|}{\xi} \right)^\nu K_\nu \left( \sqrt{2\nu} \frac{\|\boldsymbol{x}\|}{\xi} \right).$$

Hence, $C_S(\boldsymbol{x}) = M_1(\boldsymbol{x}|\xi_S, V_S)$ for both $S = H, P$. With this notation, the interspecific spatial cross-covariance function can be approximated by

$$C_{HP}(\boldsymbol{x}) \approx \int_{\mathbb{R}^2} \frac{2B_P}{A_P + B_P} \frac{K_0(\|\boldsymbol{y}\|/\xi_P)}{\xi_P^2} M_1(\boldsymbol{x} - \boldsymbol{y}|\xi_H, V_H) - \frac{2B_H}{A_H - B_H} \frac{K_0(\|\boldsymbol{y}\|/\xi_H)}{\xi_H^2} M_1(\boldsymbol{x} - \boldsymbol{y}|\xi_P, V_P) d\boldsymbol{y}.$$

## A.1 Marginal values and integrals of spatial covariance and cross-covariance functions

Following results from section A, the marginal covariance of species mean traits can be approximated via

$$C_{HP}(\boldsymbol{0}) = \frac{1}{2\pi} \int_{\mathbb{R}^2} S_{HP}(\boldsymbol{k}) d\boldsymbol{k}$$

$$\approx \frac{G_H G_P}{\sigma_H^2 \sigma_P^2} \frac{\xi_H^2 \xi_P^2}{(\xi_H^2 - \xi_P^2)^2} \left[ \frac{B_P}{N_H \sigma_H^2} \left( \xi_H^4 + \xi_H^2 \xi_P^2 (\ln \xi_P^2 - \ln \xi_H^2 - 1) \right) \right.$$

$$\left. - \frac{B_H}{N_P \sigma_P^2} \left( \xi_P^4 + \xi_H^2 \xi_P^2 (\ln \xi_H^2 - \ln \xi_P^2 - 1) \right) \right].$$

The integral correlation lengths of intraspecific phenotypic variation are given by $S_S(\boldsymbol{0})/V_S = \xi_S^2$ for $S = H, P$. This motivates the definition of an integral cross-correlation length as

$$\frac{S_{HP}(\boldsymbol{0})}{C_{HP}(\boldsymbol{0})} = \frac{1}{C_{HP}(\boldsymbol{0})} \left( - \right)$$

The integral of $C_{HP}(\boldsymbol{x})$ is approximated via

$$\int_{\mathbb{R}^2} C_{HP}(\boldsymbol{x}) d\boldsymbol{x} = 2\pi S_{HP}(\boldsymbol{0}) \approx 2\pi \left( \frac{B_P}{G_H N_H (A_H - B_H)^2 (A_P + B_P)} - \frac{B_H}{G_P N_P (A_H - B_H)(A_P + B_P)^2} \right)$$

$$= 2\pi \left( \frac{B_P V_H \xi_H^2}{A_P + B_P} - \frac{B_H V_H \xi_H^2}{A_H - B_H} \right).$$

However, the integral $\int_{\mathbb{R}^2} C_{HP}(\boldsymbol{x}) d\boldsymbol{x}$ is biased by larger distances. To see this we can change our integration to polar coordinates to find $\int_{\mathbb{R}^2} C_{HP}(\boldsymbol{x}) d\boldsymbol{x} = 2\pi \int_0^\infty C_{HP}(r) r dr$. To remove this bias, we should like to calculate $\int_0^\infty C_{HP}(r) dr$. Switching this integral back to Cartesian coordinates yields

$$\int_0^\infty C_{HP}(r) dr = \frac{1}{2\pi} \int_{\mathbb{R}^2} \frac{1}{\|\boldsymbol{x}\|} C_{HP}(\boldsymbol{x}) d\boldsymbol{x}.$$

To evaluate $\int_0^\infty C_{HP}(r) dr$, we can use the relationship

$$\int_{\mathbb{R}^2} \frac{1}{\|\boldsymbol{x}\|} C_{HP}(\boldsymbol{x}) d\boldsymbol{x} = \mathscr{F} \left\{ \frac{C_{HP}(\boldsymbol{x})}{\|\boldsymbol{x}\|} \right\}_{\boldsymbol{k}=\boldsymbol{0}},$$

where $\mathscr{F}$ denotes Fourier transformation and the subscript denotes evaluation at $\boldsymbol{k} = \boldsymbol{0} = (0,0)^\top$. Taking the Fourier transform of $C_{HP}(\boldsymbol{x})/\|\boldsymbol{x}\|$, we find

$$\mathscr{F} \left\{ \frac{C_{HP}(\boldsymbol{x})}{\|\boldsymbol{x}\|} \right\} \approx \frac{B_P}{A_P + B_P} \frac{1}{1 + \frac{1}{2}\xi_P^2 \|\boldsymbol{k}\|^2} \frac{V_H \xi_H / \sqrt{2}}{1 + \frac{1}{2}\xi_H^2 \|\boldsymbol{k}\|^2} E\left( -\frac{1}{2} \xi_H^2 \|\boldsymbol{k}\|^2 \right)$$

$$- \frac{B_H}{A_H - B_H} \frac{1}{1 + \frac{1}{2}\xi_H^2 \|\boldsymbol{k}\|^2} \frac{V_P \xi_P / \sqrt{2}}{1 + \frac{1}{2}\xi_P^2 \|\boldsymbol{k}\|^2} E\left( -\frac{1}{2} \xi_P^2 \|\boldsymbol{k}\|^2 \right),$$

where $E(\zeta) = \int_0^{\pi/2} \sqrt{1 - \zeta \sin^2 \theta} \, d\theta$ is an elliptic integral. In particular, this provides

$$\lim_{\boldsymbol{k} \to \boldsymbol{0}} \mathscr{F} \left\{ \frac{C_{HP}(\boldsymbol{x})}{\|\boldsymbol{x}\|} \right\} \approx \frac{\pi}{2} \left( \frac{B_P}{A_P + B_P} \frac{\xi_H}{\sqrt{2}} V_H - \frac{B_H}{A_H - B_H} \frac{\xi_P}{\sqrt{2}} V_P \right).$$

We therefore conclude

$$\int_0^\infty C_{HP}(r) dr \approx \frac{1}{4} \left( \frac{B_P}{A_P + B_P} \frac{\xi_H}{\sqrt{2}} V_H - \frac{B_H}{A_H - B_H} \frac{\xi_P}{\sqrt{2}} V_P \right).$$

Using the same trick to compute the integral lengths of intraspecific phenotypic variation, we find

$$\int_0^\infty C_S(r) dr = \frac{1}{2\pi} \lim_{\boldsymbol{k} \to \boldsymbol{0}} \mathscr{F} \left\{ \frac{C_S(\boldsymbol{x})}{\|\boldsymbol{x}\|} \right\} \approx \frac{V_S \xi_S}{4\sqrt{2}}.$$

The quantity $\mathscr{I}_S = \int_0^\infty C_S(r) dr$ has been referred to as the integral length of spatial covariance (here the integral length of intraspecific spatial covariance). Then, an integral length of interspecific spatial covariance may be computed as

$$\mathscr{I}_{HP} := \int_0^\infty |C_{HP}(r)| dr.$$

Assuming $C_{HP}(r)$ is either always positive or always negative allows us to move the absolute value outside of the integral. Then, under our model, we find

$$\mathscr{I}_{HP} \approx \frac{1}{4\sqrt{2}} \left| \frac{B_P}{A_P + B_P} V_H \xi_H - \frac{B_H}{A_H - B_H} V_P \xi_P \right|$$

$$= \frac{1}{4\sqrt{2}} \left| \frac{B_P}{(A_P + B_P)(A_H - B_H)^{3/2}} \frac{1}{\sigma_H \rho_H \sqrt{G_H}} - \frac{B_H}{(A_H - B_H)(A_P + B_P)^{3/2}} \frac{1}{\sigma_P \rho_P \sqrt{G_P}} \right|.$$

### A.2   Spurious spatial correlations on bounded regions

Consider the region $U$ of $\mathbb{R}^2$ such that $|U| < \infty$. Then, the covariance of mean traits on this region is given by

$$\text{Cov}_U(\bar{z}_H, \bar{z}_P) = \frac{1}{|U|} \int_U \left(\bar{z}_H(\boldsymbol{x}) - \bar{\bar{z}}_H\right)\left(\bar{z}_P(\boldsymbol{x}) - \bar{\bar{z}}_P\right)d\boldsymbol{x},$$

where $\bar{\bar{z}}_S$ is the average of $\bar{z}_S$ on the region $U$. What is the mean and variance of $\text{Cov}_U(\bar{z}_H, \bar{z}_P)$? How does the radius of $U$ relative to the dispersal rates mediate these moments? Is the calculation easier when $U$ is a disk of radius $R > 0$?

## B   Measures of local adaptation

- use $\mathcal{L}$ for measures in terms of mean fitness and $\ell$ for measures in terms of log-mean fitness

Local adaptation is commonly measured as the difference in fitness for individuals experiencing their local environment and fitness for individuals experiencing foreign environments (Gandon & Nuismer 2009, Nuismer 2017, etc). In the case of coevolution, the environmental variable is replaced by the trait value of the interacting partner species.

yada yada yada, folks end up with something like $\mathcal{L}_P = \tilde{\alpha} - \tilde{\alpha}_0$. Using a slightly different definition, parasite local adaptation simplifies to $\ell_P = \widetilde{\ln \alpha} - \widetilde{\ln \alpha_0} = B_P C_{HP}(0)$.

Here extend this notion of local adaptation to the case of populations distributed continuously in space. In particular, we denote by $\Delta_H(\boldsymbol{y})$ the difference in expected population growth rates of the host when confronted with parasites drawn from a spatial lag $\boldsymbol{y} = (y_1, y_2)^\top$ away. That is,

$$\Delta_H(\boldsymbol{y}) = \mathbb{E}[m_H(\bar{z}_H(\boldsymbol{x}), \bar{z}_P(\boldsymbol{x})) - m_H(\bar{z}_H(\boldsymbol{x}), \bar{z}_P(\boldsymbol{x} + \boldsymbol{y}))].$$

We define $\Delta_P(\boldsymbol{y})$ in a complementary manner for the parasite species. Under our model of trait matching/mismatching, $\Delta_H(\boldsymbol{y})$ simplifies to

$$\Delta_H(\boldsymbol{y}) = \mathbb{E}\left[\frac{B_H}{2}\left(\bar{z}_H(\boldsymbol{x}) - \bar{z}_P(\boldsymbol{x})\right)^2 - \frac{B_H}{2}\left(\bar{z}_H(\boldsymbol{x}) - \bar{z}_P(\boldsymbol{x} + \boldsymbol{y})\right)^2\right] = -B_H C_{HP}(\boldsymbol{y}).$$

Similarly, we obtain $\Delta_P(\boldsymbol{y}) = B_P C_{HP}(\boldsymbol{y})$ for the parasite. To provide a global measure of local adaptation, one that accounts for all spatial distances, we might think $\hat{\ell}_S = \int_{\mathbb{R}^2} \Delta_S(\boldsymbol{y})d\boldsymbol{y}$ would provide a reasonable definition. Using our results from section A, we obtain

$$\hat{\ell}_H \approx B_H\left(\frac{B_H}{G_P N_P(A_H - B_H)(A_P + B_P)^2} - \frac{B_P}{G_H N_H(A_H - B_H)^2(A_P + B_P)}\right),$$

$$\hat{\ell}_P \approx B_P\left(\frac{B_P}{G_H N_H(A_H - B_H)^2(A_P + B_P)} - \frac{B_H}{G_P N_P(A_H - B_H)(A_P + B_P)^2}\right).$$

These measures of local adaptation depend on the effective densities $N_H, N_P$ which suggests they provide some indication for the role of random genetic drift in determining global patterns of local adaptation. However, they are not dependent on dispersal distances because of the extra weight given to larger distances implicit in this definition (see above). Hence, they provide no information on the role of gene-flow in determining global patterns of local adaptation. To circumvent this issue, we define another index $\tilde{\ell}_S = \int_0^\infty \tilde{\Delta}_S(r)dr$ where $\tilde{\Delta}_S(r) = \Delta_S(\boldsymbol{r})$ and $\boldsymbol{r} = (r/\sqrt{2}, r/\sqrt{2})$. Using our results from above, we find

$$\tilde{\ell}_H \approx \frac{B_H}{4}\left(\frac{B_H}{A_H - B_H}\frac{\xi_P}{\sqrt{2}} - \frac{B_P}{A_P + B_P}\frac{\xi_H}{\sqrt{2}}\right),$$

$$\tilde{\ell}_P \approx \frac{B_P}{4}\left(\frac{B_P}{A_P + B_P}\frac{\xi_H}{\sqrt{2}} - \frac{B_H}{A_H - B_H}\frac{\xi_P}{\sqrt{2}}\right).$$

Since $\xi_S \propto \sigma_S$ for $S = H, P$ we see that this alternative global index of local adaptation captures the role of gene-flow. However, the absence effective densities in these expressions suggests $\tilde{\ell}_H, \tilde{\ell}_P$ do not capture the effects of random genetic drift. Hence, the two sets of indices $(\hat{\ell}_H, \ell_P)$ and $(\tilde{\ell}_H, \tilde{\ell}_P)$ capture complementary aspects of global patterns of local adaptation in coevolving hosts and parasites.

In particular, they both measure adaptation of a host (resp parasite) when confronted with a randomly sampled parasite (resp host) drawn from a randomly chosen location. However, the spatial sampling scheme differs between the two. While $\hat{\ell}$ samples space uniformly in two-dimensions, $\tilde{\ell}$ samples space uniformly along a transect. Hence, while $\hat{\ell}$ captures orientation, it is sensitive to spatial dimension. In contrast, $\tilde{\ell}$ focuses on the effect of distance and we therefore focus on results for $\tilde{\ell}$ in the main text.

curious: does $\hat{\ell}$ match the conditions for winner/loser in the case of stochastic evolution without a spatial component?

## B.1    Modified Index of Local Adaptation Accounting for Limited Dispersal

We denote by $D(\boldsymbol{x})$ the probability density that two individuals of opposing species were separated by $\boldsymbol{x}$ before dispersal given that they end up at the same location after dispersal. We refer to $D(\boldsymbol{x})$ as the separation kernel. Since we assume dispersal for each species is bivariate Gaussian with respective standard deviations (in both coordinates) $\sigma_H, \sigma_P$, $D(\boldsymbol{x})$ will also be bivariate Gaussian with standard deviation $\sqrt{\sigma_H^2 + \sigma_P^2}$.

Whereas local adaptation is classically measured as the difference between fitness "at home" versus fitness in a randomly selected environment, the limited dispersal analog is fitness "at home" versus fitness in a randomly selected environment weighted by the separation kernel. In particular, for species $S = H, P$,

$$\hat{\mathcal{L}}_S = \mathbb{E}[\bar{w}_S(\boldsymbol{x}, \boldsymbol{x})] - \mathbb{E}\left[\int_{\mathbb{R}^2} \bar{w}_S(\boldsymbol{x}, \boldsymbol{x}+\boldsymbol{y})D(\boldsymbol{y})d\boldsymbol{y}\right],$$

where $\bar{w}_H(\boldsymbol{x}, \boldsymbol{y})$ and $\bar{w}_P(\boldsymbol{x}, \boldsymbol{y})$ are shorthand for $\bar{w}_H(\bar{z}_H(\boldsymbol{x}), \bar{z}_P(\boldsymbol{y}))$ and $\bar{w}_P(\bar{z}_P(\boldsymbol{x}), \bar{z}_H(\boldsymbol{y}))$ respectively. Applying the trait matching/mis-matching model of fitness, we obtain

$$\hat{\mathcal{L}}_H = \cdots$$

$$\hat{\mathcal{L}}_P = \cdots$$

For the sake of clarity, we focus on a closely related measure of local adaptation that utilizes the local population growth rate $\bar{m}_S$ instead of the population mean fitness $\bar{w}_S$ for species $S = H, P$. In particular, we define

$$\hat{\ell}_S = \mathbb{E}[\bar{m}_S(\boldsymbol{x}, \boldsymbol{x})] - \mathbb{E}\left[\int_{\mathbb{R}^2} \bar{m}_S(\boldsymbol{x}, \boldsymbol{x}+\boldsymbol{y})D(\boldsymbol{y})d\boldsymbol{y}\right],$$

where $\bar{m}_H(\boldsymbol{x}, \boldsymbol{y})$ and $\bar{m}_P(\boldsymbol{x}, \boldsymbol{y})$ are shortand for $\bar{m}_H(\bar{z}_H(\boldsymbol{x}), \bar{z}_P(\boldsymbol{y}))$ and $\bar{m}_P(\bar{z}_P(\boldsymbol{x}), \bar{z}_H(\boldsymbol{y}))$ respectively. Applying the trait matching/mis-matching model of fitness along with our assumption of spatially homogeneous abiotic stabilizing selection, we obtain

$$\mathbb{E}[\bar{m}_H(\boldsymbol{x}, \boldsymbol{x})] = r_H - \frac{A_H}{2}[(\theta_H - \mu_H)^2 + v_H + V_H] + \frac{B_H}{2}[(\mu_H - \mu_P)^2 + v_H + v_P + V_H + V_P]$$
$$- B_H C_{HP}(0), \quad (14)$$

$$\mathbb{E}\left[\int_{\mathbb{R}^2} \bar{m}_H(\boldsymbol{x}, \boldsymbol{y})D(\boldsymbol{y})d\boldsymbol{y}\right] = r_H - \frac{A_H}{2}[(\theta_H - \mu_H)^2 + v_H + V_H]$$
$$+ \frac{B_H}{2}[(\mu_H - \mu_P)^2 + v_H + v_P + V_H + V_P] - B_H \int_{\mathbb{R}^2} C_{HP}(\boldsymbol{y})D(\boldsymbol{y})d\boldsymbol{y}, \quad (15)$$

$$\mathbb{E}[\bar{m}_P(\boldsymbol{x}, \boldsymbol{x})] = r_P - \frac{A_P}{2}[(\theta_P - \mu_P)^2 + v_P + V_P] - \frac{B_P}{2}[(\mu_P - \mu_H)^2 + v_P + v_H + V_P + V_H]$$
$$+ B_P C_{HP}(0), \quad (16)$$

$$\mathbb{E}\left[\int_{\mathbb{R}^2} \bar{m}_P(\boldsymbol{x}, \boldsymbol{y})D(\boldsymbol{y})d\boldsymbol{y}\right] = r_P - \frac{A_P}{2}[(\theta_P - \mu_P)^2 + v_P + V_P]$$
$$- \frac{B_P}{2}[(\mu_P - \mu_H)^2 + v_P + v_H + V_P + V_H] + B_P \int_{\mathbb{R}^2} C_{HP}(\boldsymbol{y})D(\boldsymbol{y})d\boldsymbol{y}, \quad (17)$$

Setting $\bar{C}_{HP} \int_{\mathbb{R}^2} C_{HP}(\boldsymbol{y})D(\boldsymbol{y})d\boldsymbol{y}$, the expressions for local adaptation accounting for limited dispersal simplify to

$$\hat{\ell}_H = B_H \left( \bar{C}_{HP} - C_{HP}(0) \right),$$

$$\hat{\ell}_P = B_P \left( C_{HP}(0) - \bar{C}_{HP} \right).$$

## B.2 Scott's measure of coevolutionary advantage

$$a = \bar{\bar{m}} - \bar{\bar{m}}^0$$

where $\bar{\bar{m}}^0$ is the spatial average of growth rate in the absence of biotic selection. Setting $\bar{\bar{z}}_S^0, V_S^0$ the spatial mean and variance of local mean traits for species $S$ and $C_{HP}^{S,0}$ the covariance of mean traits between species when $B_S = 0$, our model assumptions then implies

$$a_P = B_P(C_{HP} - C_{HP}^{P,0}) - \frac{B_P}{2}\left[(\bar{\bar{z}}_H - \bar{\bar{z}}_P)^2 + V_H + V_P + v_H + v_P\right]$$
$$- \frac{A_P}{2}\left[(\theta_P - \bar{\bar{z}}_P)^2 - (\theta_P - \bar{\bar{z}}_P^0)^2 + V_P - V_P^0\right], \quad (18)$$

$$a_H = -B_P(C_{HP} - C_{HP}^{H,0}) + \frac{B_H}{2}\left[(\bar{\bar{z}}_P - \bar{\bar{z}}_H)^2 + V_H + V_P + v_H + v_P\right]$$
$$- \frac{A_H}{2}\left[(\theta_H - \bar{\bar{z}}_H)^2 - (\theta_H - \bar{\bar{z}}_H^0)^2 + V_H - V_H^0\right]. \quad (19)$$

- NOTE: Scott defines this measure by comparing the coevolutionary scenario to the no biotic selection for both species scenario. In this case it seems possible that $a$ can be positive for both species, blurring the distinction of which species is "winning" the coevolutionary race. Alternatively, we can proceed as above and consider the case when just one or the other species incurs zero biotic selection.

## B.3 Relation to results derived without gene-flow

Expressions for the spatial means, variance and covariance of local mean traits across a set of discrete populations without gene-flow between them have been presented by Week & Nuismer (2019). In the model of Week & Nuismer (2019) coevolution was driven by an offset-matching mechanism to capture trait escalation. When a parameter of their model known as the optimal offset is set to zero, the classical trait-matching model is recovered. Here we show how the results of Week & Nuismer (2019) on the spatial moments of a discrete space model with zero optimal offset are recovered as a special case of the SPDE model presented here in the limit of zero gene-flow (that is, in the limit of $\sigma_H, \sigma_P \to 0$). In this limit our SPDE model becomes

$$\dot{z}_H = G_H A_H(\theta_H - \bar{z}_H) - G_H B_H(\bar{z}_P - \bar{z}_H) + \sqrt{\frac{G_H}{N_H}}\dot{W}_H,$$

$$\dot{\bar{z}}_P = G_P A_P (\theta_P - \bar{z}_P) + G_P B_P (\bar{z}_H - \bar{z}_P) + \sqrt{\frac{G_P}{N_P}} \dot{W}_P.$$

Without the homogenizing action of diffusive movement, solutions to this equation become more technically involved. In particular, we no longer have a function-valued equilibrium solution $(\bar{z}_H, \bar{z}_P)^\top$. Instead, we work a more general notion called a measure-valued solution. Whereas the function-valued solution takes points in $\mathbb{R}^2$ and returns normally distributed random variables, the measure-valued solution takes subsets of $\mathbb{R}^2$ and returns normally distributed random variables.

To provide intuition for the measure-valued solutions, let us first consider the case where $\sigma_H, \sigma_P > 0$ so that the equilibrium function-valued solution $(\bar{z}_H, \bar{z}_P)^\top$ does in fact exist. Then for bounded regions $U$ of $\mathbb{R}^2$ we can define

$$\bar{Z}_H(U) = \frac{1}{|U|} \int_U \bar{z}_H(x)dx, \quad \bar{Z}_P(U) = \frac{1}{|U|} \int_U \bar{z}_P(x)dx,$$

where $|U|$ denotes the area of the region $U \subset \mathbb{R}^2$. In this way, both $\bar{Z}_H$ and $\bar{Z}_P$ are random measures on subsets of $\mathbb{R}^2$ and thus constitute an equilibrium measure-valued solution of the SPDE model.

Although the function-valued solution $(\bar{z}_H, \bar{z}_P)^\top$ fails to exist in the absence of gene-flow ($\sigma_H, \sigma_P = 0$), a measure-valued solution $(\bar{Z}_H, \bar{Z}_P)^\top$ does exist. In fact, for each fixed $U \subset \mathbb{R}^2$ such that $|U| < \infty$, $(\bar{Z}_H(U), \bar{Z}_P(U))^\top$ correspond to equilibrium solutions of a bivariate Ornstein-Uhlenbeck process. Following results presented in Vatiwutipong and Phewchean (2019), the distribution of $(\bar{Z}_H(U), \bar{Z}_P(U))^\top$ is bivariate normal determined by the mean vector $\boldsymbol{\mu} = (\mu_H, \mu_P)^\top$ with

$$\mu_H = \frac{(A_P + B_P)A_H \theta_H - B_H A_P \theta_P}{(A_P + B_P)A_H - B_H A_P},$$

$$\mu_P = \frac{(A_H - B_H)A_P \theta_P + B_P A_H \theta_H}{(A_H - B_H)A_P + B_P A_H},$$

and variance-covariance matrix $\boldsymbol{\Sigma} = \left( \begin{smallmatrix} V_H & C_{HP} \\ C_{HP} & V_P \end{smallmatrix} \right)$ with

$$V_H = \frac{\frac{1}{2N_H} - B_H C_{HP}}{A_H - B_H}, \quad V_P = \frac{\frac{1}{2N_P} + B_P C_{HP}}{A_P + B_P}$$

$$C_{HP} = \frac{B_P(A_P + B_P)G_P N_P - B_H(A_H - B_H)G_H N_H}{2(A_H A_P + A_H B_P - A_P B_H)((A_H - B_H)G_H + (A_P + B_P)G_P)N_H N_P}.$$

This results correspond to the results found by Week & Nuismer (2019) when the optimal offset is set to zero. Hence, the statistical model of Week & Nuismer (2019) can be interpreted as a special case of the continuous space model presented here in the limit of zero gene-flow. Assuming weak coevolution so that $B_H^2, B_P^2, B_H B_P \approx 0$, we recover the marginal variances of mean trait values found using the SPDE with gene-flow. However, applying the same approximation to the covariance $C_{HP}$ does not return the marginal covariance found using the SPDE model with gene-flow. Hence, the presence of gene-flow and limited dispersal fundamentally alters patterns of spatial trait covariance between coevolving species.

## C   The individual-based model

# References

Bezanson, Jeff, Alan Edelman, Stefan Karpinski, and Viral B Shah. 2017. "Julia: A Fresh Approach to Numerical Computing." *SIAM Review* 59 (1): 65–98. https://doi.org/10.1137/141000671.

Bjørnstad, Ottar N., and Jordi Bascompte. 2001. "Synchrony and Second-Order Spatial Correlation in Host-Parasitoid Systems." *Journal of Animal Ecology* 70 (6): 924–33. https://doi.org/10.1046/j.0021-8790.2001.00560.x.

Vatiwutipong, P., and N. Phewchean. 2019. "Alternative Way to Derive the Distribution of the Multivariate Ornstein-Uhlenbeck Process." *Advances in Difference Equations* 2019 (1). https://doi.org/10.1186/s13662-019-2214-1.